The Formation of CCBO and $[CCBO]^+$ from $[CCBO]^-$ in the Gas Phase: A Joint Experimental and Theoretical Study

Andrew M. McAnoy,[†] Suresh Dua,[†] Detlef Schröder,[‡] John H. Bowie,*[,†] and Helmut Schwarz[‡]

Department of Chemistry, The University of Adelaide, South Australia 5005, Australia, and Institut für Chemie, Technische Universität Berlin, D-10623 Berlin, Germany

Received: June 25, 2002; In Final Form: December 2, 2002

The stable anion $[CCBO]^-$ may be formed in the chemical ionization source of a mass spectrometer by the process $F^- + (CH_3)_3Si-C\equiv C-B(O\text{-}iso\text{-}Pr)_2 \rightarrow [CCBO]^- + (CH_3)_3SiF + CH_3-CH=CH_2$. Anion $[CCBO]^-$ may be converted to stable doublet CCBO by a collision-induced vertical Franck−Condon oxidation in the first of two collision cells. Calculations at the MP4SDTQ/aug-cc-pVTZ//MP2(full)/6-31G(d) level of theory indicate that $[CCBO]^-$ and CCBO are linear species, with structures approximated by valence bond forms $[:C=C=B=O]^-$ and $\cdot C\equiv C-B=O$, respectively. Neutral CCBO may be converted to $[CCBO]^+$ in the second collision cell by vertical ionization. Some of the $[CCBO]^+$ cations are stable, while others are energized and undergo rearrangement to $[OCCB]^+$. This exothermic rearrangement may occur for both the singlet and triplet forms of $[CCBO]^+$ (the triplet form is lower in energy by only 5.2 kcal mol^{-1}) with both rearrangements proceeding through distorted rhombic forms of [*cyclo*-CCBO]$^+$.

Introduction

Carbon clusters (cumulenes) have been studied in great detail because of their importance in flame chemistry and astrochemistry.[1] In contrast, studies on similar compounds containing boron and carbon have been concentrated on borocumulenes with boron occupying a terminal position in such molecules. An early mass spectrometric study showed strong bonding between carbon and boron.[2] Since that time, a number of studies have involved heating boron/carbon mixtures at high temperatures or by laser irradiation of carbon/boron layers on metal surfaces. The products of these processes are generally trapped in low-temperature matrixes (e.g., solid argon), and the structures of the major products determined using various spectroscopic methods including infrared spectroscopy and electron spin resonance spectroscopy. The following species have been reported: (i) the anion, neutral, and cation of BC;[3−9] (ii) neutral BC_2 of which the cyclic form is some 6 kcal mol^{-1} lower in energy than the linear structure,[10−12] linear BC_2^-,[9,13−15] and cyclic BC_2^+;[16] (iii) linear BC_3^- and linear BC_3,[17] and rhombic BC_3^+;[16] (iv) linear BC_4^- [13] and cyclic BC_4^+;[16] (v) bent (distorted "linear") BC_n^- ($n = 5-13$);[13] (vi) linear BCCB;[17] and (vii) various species containing B, CO, and O, e.g., BCO, $B(CO)_2$, $(CBO)_2$[14,18−20] and $C_{2n}BO^-$ [($n = 1-5$); no data concerning the structures are available].[14]

Our interest in borocumulenes follows our earlier studies of cumulenes, e.g. the formation of neutral linear and rhombic C_4,[21] and our earlier report of the formation of the anions $[CH_2=B=CH_2]^-$ and $[CH_2=B=O]^-$.[22] Our approach to the generation of transient neutrals in the mass spectrometer is collision-induced vertical oxidation of mass selected anions of known bond connectivity by means of the neutralization/reionization (NR) procedure.[23−25] In this respect it is of prime importance that the anions under study are in turn formed from precursors with well-defined, known structures, e.g. ref 21.

This paper addresses two questions, namely, (i) can the CCBO neutral be formed from linear $[CCBO]^-$ by the neutralization/reionization (NR) procedure? and (ii) does neutral CCBO rearrange under the conditions of the NR experiment, and, if so, what is the product and what is the mechanism of the rearrangement?

Experimental Section

A. Mass Spectrometric Methods. The experiments were performed using a modified HF-ZAB/AMD 604 four-sector mass spectrometer with BEBE configuration,[24] where B and E represent magnetic and electric sectors, respectively. The $[CCBO]^-$ anion was generated by chemical ionization (CI) in the negative ion mode, with typical source conditions as follows: source temperature 200 °C, repeller voltage −0.5 V, ion extraction voltage 8 kV, mass resolution $m/\Delta m \geq 1500$. $(CH_3)_3Si-C\equiv C-B(O\text{-}iso\text{-}Pr)_2$ was placed in a small glass capillary tube which was then drawn out in a flame to create a very fine aperture, allowing for a slow steady release of sample vapor upon heating. The capillary was inserted into the CI source via the direct probe; the probe tip was heated to 60−80 °C to generate a background pressure of ca. 10^{-5} Torr inside the source housing. The $[CCBO]^-$ anion was formed following desilylation,[26] (followed by fragmentation as shown in Scheme 1) utilizing SF_6 as a CI reagent gas at a pressure of ca. 10^{-4} Torr inside the source housing. This is similar to the method first introduced by Squires and co-workers using F_2/NF_3 mixtures.[27]

Collision induced dissociation (CID) of B(1)-mass selected ions was effected in collision cells positioned between B(1) and E(1). Helium was used as a target gas. The pressure of the collision gas in the cell was maintained such that 80% of the parent ion beam was transmitted through the cell. This corresponds to an average of 1.1−1.2 collisions per ion.[28] Product ions resulting from CID were recorded by scanning E(1).

Neutralization−reionization[23,24] ($^-NR^+$) experiments were performed for B(1)-mass selected $[C_2BO]^-$ utilizing the dual collision cells located between sectors B(1) and E(1). Neutral-

* Corresponding author. Department of Chemistry, The University of Adelaide, South Australia 5005. E-mail: john.bowie@adelaide.edu.au.
† Department of Chemistry.
‡ Institut für Chemie.

10.1021/jp0214920 CCC: $25.00
Published on Web 02/01/2003

SCHEME 1

$$F^- + (CH_3)_3Si\text{-}C{\equiv}C\text{-}B(O\text{-}iso\ Pr)_2 \rightarrow (CH_3)_3SiF + {}^-C{\equiv}C\text{-}B(O\text{-}iso\ Pr)_2 \quad (1)$$

$$^-C{\equiv}C\text{-}B(O\text{-}iso\ Pr)_2 \rightarrow [(:C{=}C{=}B\text{-}O\text{-}iso\ Pr)\ ^-O\text{-}iso\ Pr] \rightarrow [CCBO]^- + iso\ PrOH + CH_3CH{=}CH_2 \quad (2)$$

ization of the anions was achieved by collisional electron detachment using O_2 at 80% transmittance as collision gas, while reionization to cations was achieved by collision of the neutrals with O_2, again at 80% transmittance. Any ions remaining after the first collision event were deflected from the primary neutral beam using an electrode maintained at a high voltage (1 kV) positioned before the second collision cell. To detect a recovery signal due to the reionized parent molecule, the neutral species must be stable for approximately one microsecond. Charge reversal ($^-CR^+$) spectra[29−31] were recorded near single-collision conditions (O_2, 80% T). Collection of $^-CR^+$ and $^-NR^+$ spectra under the same experimental conditions allows for a direct comparison to be made from which it is possible to infer the behavior of the intermediate neutral on the NR time scale (10^{-6} s).[24,32,33]

B. Synthesis of 1-Trimethylsilylethylyldiisopropoxyborane. (1-Trimethylsilylethynlyl)diisopropoxyborane was prepared using a modification of a reported procedure.[34,35] Trimethylsilylacetylene (4.2 cm^3, 29.7 mmol) in anhydrous diethyl ether (30 cm^3) was cooled to −78 °C under nitrogen, and *n*-butyllithium in hexane (12.5 cm^3, 30.0 mmol) was added over a period of 30 min. The organolithium reagent was then slowly added at −78 °C to triisopropyl borate (7.0 cm^3, 29.7 mmol) in diethyl ether (15.0 cm^3), and the reaction was maintained at −78 °C for 2 h. Anhydrous hydrogen chloride in diethyl ether (2.0M, 15.0 cm^3, 30.0 mmol) was added, and the mixture was allowed to warm to 20 °C. The LiCl was removed by centrifugation and the remaining solvent removed in vacuo. Distillation of the residue at 80 °C/7 mm Hg gave the title compound (4.8 g, 70% yield). ^1H NMR (500 MHz, in $CDCl_3$) δ: 0.19 (s, 9H), 1.16 (d, 2 × 6H, J = 6.1), 4.56 (septet, 2 × 1H, J = 6.1).

C. Theoretical Methods. All geometry optimizations were carried out at the MP2(full)/6-31G(d) level of theory using the GAUSSIAN 98 suite of programs.[36] Stationary points were characterized as either minima (no imaginary frequencies) or transition structures (one imaginary frequency) by calculation of the frequencies using analytical gradient procedures. The minima connected by a given transition structure were confirmed by intrinsic reaction coordinate (IRC) calculations. The calculated frequencies were also used to determine zero-point vibrational energies which were then scaled by 0.9661[37] and used as a zero-point correction for the electronic energies calculated at higher levels of theory. The energies of these geometries were determined in single-point calculations at the MP4SDTQ level using the Dunning aug-cc-pVTZ basis set.[38,39] All calculations were carried out on the Alpha server at the APAC National Facility (Canberra).

Results and Discussion

Since the primary target of this study is the generation of CCBO from the negative ion $[CCBO]^-$, let us investigate whether the neutral and anion of this connectivity are stable species from a theoretical viewpoint. First, we determine which neutral BC_2O isomers are local minima on the BC_2O potential surface.

The Formation of $[CCBO]^-$. There are 13 stable doublet BC_2O isomers listed in Scheme 2. Only bond connectivities and

SCHEME 2

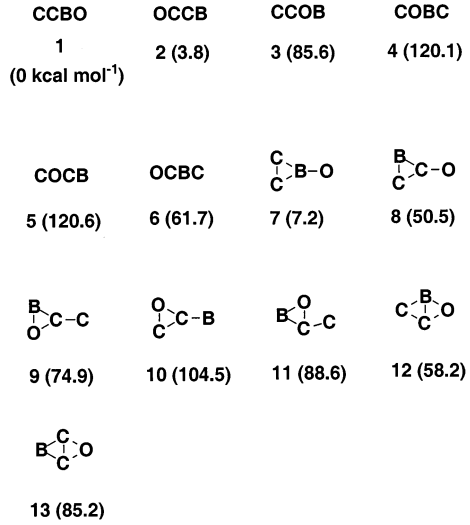

relative energies are shown in Scheme 2; full details of each isomer are given in Table 1. Geometries were calculated at the MP2(full)/6-31G(d) level of theory with the energies determined at the MP4SDTQ/aug-cc-pVTZ//MP2(full)/6-31G(d) level of theory. The target neutral CCBO is the global minimum on the potential surface. Other low energy isomers are OCCB [**2**, +3.8 kcal mol^{-1} relative to CCBO (**1**, 0 kcal mol^{-1})] and the cyclic system **7** (+7.2 kcal mol^{-1}). The other 10 isomers are 50−120 kcal mol^{-1} higher in energy than **1**; for example, the two distorted rhombic forms (**12** and **13**) have the relative energies +58.2 and + 85.2 kcal mol^{-1}, respectively.

Having established that neutral CCBO is stable, we now need to ascertain whether anion $[CCBO]^-$ is an appropriate precursor for this neutral. Is $[CCBO]^-$ stable, or does it rearrange to an isomeric structure in the keV collisions involved in the vertical Franck−Condon oxidation? If $[CCBO]^-$ rearranges, then it is not appropriate for use in the vertical oxidation to CCBO. The results of theoretical calculations to determine the geometries and energies of stable anionic isomers of BC_2O are summarized in Table 2.

Theory predicts twelve minima on the BC_2O anion potential surface. There are seven singlet anions and five triplets (Table 2). The global minimum corresponds to singlet $[CCBO]^-$, the target of our planned gas-phase synthesis. There is a triplet form of $[CCBO]^-$, but it is 111.6 kcal mol^{-1} more positive in energy than the singlet. The isomer closest in energy to singlet $[CCBO]^-$ is singlet $[OCCB]^-$, which lies 53.5 kcal mol^{-1} above singlet $[CCBO]^-$. Even though it is unlikely that $[OCCB]^-$ could be accessible from $[CCBO]^-$ during collisional activation, this is a process which needs to be studied from an experiment viewpoint. The other eight $[BC_2O]^-$ isomers are in the range 71−174 kcal mol^{-1} above singlet $[CCBO]^-$. Although some of these structures are of interest in their own right, they will not be accessible from $[CCBO]^-$, and are not considered further.

Singlet $[CCBO]^-$ is linear, and best represented by the valence bond structure $[:C{=}C{=}B{=}O]^-$: the extra electron is involved in the multiple bonding around boron. Electron delocalization is also implied by the C−C distance of 1.27 Å, which is longer than the bond distance in acetylene (1.18 Å). In contrast, although the bond lengths of triplet $[CCBO]^-$ are very similar to those of the singlet, the triplet is significantly bent giving trans type geometry, with each of the CCB and CBO angles close to 168°.

We conclude from the computational study that singlet $[CCBO]^-$ should be a viable precursor for neutral CCBO.

TABLE 1: Minima Located on the BC_2O Neutral Potential Energy Surface

	C_1C_2BO	OC_1C_2B	C_1C_2OB	C_1OBC_2	C_1OC_2B	OC_1BC_2	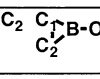	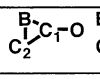		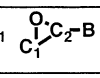	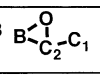		
	1	**2**	**3**	**4**	**5**	**6**	**7**	**8**	**9**	**10**	**11**	**12**	**13**
State	$^2\Sigma$	$^2\Sigma$	$^2A'$	$^2\Sigma$	$^2\Sigma$	$^2\Sigma$	$^2A_1$	$^2A'$	$^2A'$	$^2A'$	n/a	$^2A'$	$^2A_1$
Symmetry	$C_{\infty v}$	$C_{\infty v}$	C_s	$C_{\infty v}$	$C_{\infty v}$	$C_{\infty v}$	C_{2v}	C_s	C_s	C_s	C_1	C_s	C_{2v}
Rel. Energy (kcal mol^{-1})	0.0[a]	3.8	85.6	120.1	120.6	61.7	7.2	50.5	74.9	104.5	88.6	58.2	85.2
Dipole Moment (Debye)	3.91	2.15	1.66	3.22	2.71	0.71	4.02	1.60	2.53	2.11	2.08	1.91	0.87
AEA (eV)[b]	4.8	2.6	4.4			4.4	-0.9	3.4	3.7	3.0		2.7	
AIE (eV)[c]	12.6	12.9					14.4					14.8	
Bond Lengths (Å)[d]													
C_1C_2	1.1822	1.2933	1.1786				1.2906	1.5675	1.3029	1.4595	1.3553	1.3217	1.5048
C_2B	1.4907	1.3403		1.2924	1.3042	1.3458	1.6835	1.4007	1.5102	1.3442	1.5252	1.4542	1.4576
C_1B						1.4334						1.6431	
BO	1.2174		1.3139	1.3991			1.2173		1.3316		1.3749	1.4024	
C_1O		1.1730		1.1749	1.1651	1.1634		1.1851		1.2984		1.4528	1.4128
C_2O			1.3022		1.3284								
Angles (°)[b]													
C_1C_2O			178.56										
C_2OB			154.96										
C_1C_2B							67.46	61.00	163.32	164.68	90.46	72.41	
C_2BO							157.46		63.34		74.29	106.38	
C_2C_1O								138.81		65.62	70.62	110.97	
BOC_1											84.64	70.24	
BC_1O													116.75
C_1OC_2													64.36
C_1BC_2													62.15
OBC_2C_1											-51.93		

[a] −175.904292 hartrees. Energy calculated at UMP4STDQ/aug-cc-pVTZ//UMP2(full)/6-31G(d) level of theory including scaled (0.9661[37]) zero-point correction. [b] Adiabatic electron affinity. [c] Adiabatic ionization energy. [d] UMP2(full)/6-31G(d) level of theory.

TABLE 2: Geometries and Relative Energies of the $[BC_2O]^-$ Anions

	C_1C_2BO	OC_1C_2B	C_1C_2OB	OC_1BC_2	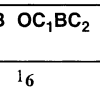			C_1C_2BO	OC_1C_2B	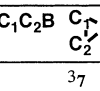	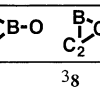	
	^{1}**1**	^{1}**2**	^{1}**3**	^{1}**6**	^{1}**8**	^{1}**9**	^{1}**10**	^{3}**1**	^{3}**2**	^{3}**7**	^{3}**8**	^{3}**12**
State	$^1\Sigma$	$^1\Sigma$	$^1\Sigma$	$^1\Sigma$	$^1A'$	$^1A'$	$^1A'$	$^3A'$	$^3A'$	$^3B_2$	$^3A'$	$^3A''$
Symmetry	$C_{\infty v}$	$C_{\infty v}$	$C_{\infty v}$	$C_{\infty v}$	C_s	C_s	C_s	C_s	C_s	C_{2v}	C_s	C_s
Rel. Energy (kcal mol^{-1})	0.0	53.5	95.4	71.0	81.2	100.2	146.3	111.6	109.0	138.3	106.9	173.6
Bond Lengths (Å)[b]												
C_1C_2	1.2690	1.2793	1.2662		1.5946	1.2691	1.3816	1.2551	1.2610	1.2709	1.4060	1.4234
C_2B	1.4468	1.4372		1.4091	1.4245		1.4640	1.4444	1.4162	1.5981	1.4895	1.6196
C_1B				1.4061	1.4543	1.8566				1.5981	1.5949	1.6196
BO	1.2422		1.2752			1.3465		1.2612				1.4584
C_1O		1.2145	1.3537	1.2092	1.2138	1.4262	1.3773		1.2270		1.2376	1.7205
C_2O							1.562					1.7205
Angles (°)[b]												
C_1C_2O					133.86	179.01	68.99		179.94		153.00	65.56
BC_2C_1					57.26		167.78	168.54	170.04	64.34	66.77	63.93
C_2BO								168.41		154.34		67.73
C_2OB						84.02						
C_1C_2BO												78.44

[a] −176.07951 hartrees. Energy calculated at MP4STDQ/aug-cc-pVTZ//MP2(full)/6-31G(d) level of theory including scaled (0.9661[37]) zero-point correction. [b] MP2(full)/6-31G(d) level of theory.

Generation of the target anion $[CCBO]^-$ in the chemical ionization source of the mass spectrometer was effected as shown in Scheme 1 (Experimental Section). The S_N2 (Si) reaction[26] between F^- and the trimethyl silyl protected ethinyl borate forms the acetylide anion shown in eq 1. A possible rationale of the overall sequence is that the parent anion cleaves to yield the ion molecule intermediate [(CCBO-*iso*-Pr) $^-$O-*iso*-Pr] (sequence 2, Scheme 1) with the iso-propoxide anion effecting an elimination reaction on the neutral to yield the products shown in sequence 2.[40] This synthetic sequence proceeds smoothly in the chemical ionization source, forming the required anion $[CCBO]^-$ with known bond connectivity.

The CA mass spectrum of anion $[CCBO]^-$ shows minimal fragmentation. The only fragment peaks in this spectrum are due to losses of C and C_2 from the parent anion in the abundance ratio ca. 1:20. The process giving CC + BO^- (+161.0 kcal

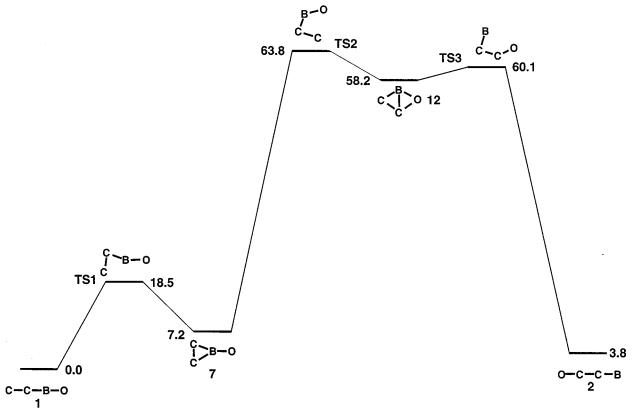

Figure 1. Theoretical calculations at the UMP4STDQ/aug-cc-pVTZ//UMP2(full)/6-31G(d) level of theory for the interconversion of CCBO (**1**) to OCCB (**2**) and to cyclo-C_2BO (**6**). Full structural details are recorded in Tables 2 and 3.

mol^{-1}) is observed, whereas that giving $CC^{-\bullet}$ + BO (+151.3 kcal mol^{-1}) is not. This is an unusual and wholly unexpected result. Perhaps there is a barrier (or bottleneck) for the process $CCBO^- \rightarrow CC^{-\bullet}$ + BO. Dissociation energies for other possible decompositions of $[CCBO]^-$ are listed in Table 6 (Supporting Information).

If anion $[CCBO]^-$ had rearranged to $[OCCB]^-$, the loss of CO would have been observed in this spectrum: a reaction endothermic by 124 kcal mol^{-1} (see Table 6). No such fragmentation is noted. We conclude that the anion product formed by the synthesis shown in Scheme 1 is $[CCBO]^-$ and that it does not rearrange under conditions equivalent to those necessary to effect the one-electron oxidation to form the neutral.

The Neutralization of $[CCBO]^-$ to Form Neutral CCBO. The next stage of the investigation is to convert the anion to neutral CCBO, and then to ionize that neutral to the corresponding cation whose fragmentation may be used as a probe to test the structure of the neutral. Theory is now used to investigate whether the required doublet neutral CCBO can be formed by Franck−Condon vertical oxidation from $[CCBO]^-$ or whether it is unstable under the reaction conditions and either rearranges to an isomeric neutral or dissociates.[41]

How many of the isomeric structures shown in Scheme 1 and Table 1 could be accessible from $[CCBO]^-$ following vertical Franck−Condon oxidation to form CCBO? Comparison of the energies of CCBO and of that neutral with the precise geometry of the anion on the neutral potential surface indicates that vertical oxidation of $[CCBO]^-$ will produce neutral CCBO with excess (Franck−Condon) energy of 10.7 kcal mol^{-1}. This is of course a minimum energy since there are other avenues to impart excess energy to the neutral, including (i) some of the excess energy of formation of the anion might be transferred to the neutral, and (ii) some neutrals may have additional excess energy as a consequence of keV collisions of the first-formed neutral in the collision cell. There are two other low-energy structures, OCCB (**2**, +3.8 kcal mol^{-1}) and the symmetrical three membered ring system **7** (+7.2 kcal mol^{-1}) that have energies less than the Franck−Condon excess energy (10.7 kcal mol^{-1}), and, in principle, may be accessible from energized CCBO provided that the barriers of these processes can be surmounted.

The results of theoretical studies for the interconversion of CCBO (**1**) to OCCB (**2**) and to **7** are summarized in Figure 1, with full details of neutrals and transition states recorded in Tables 2 and 3, respectively. There is a channel for conversion of CCBO to OCCB via **7** (+7.2 kcal mol^{-1}) and cyclic

TABLE 3: Transitation States on the Neutral Potential Energy surface

	$C_1^{C_2}B_O$	$C_2^{B-O}C_1$	$C_2^{B}C_1^{O}$
	TS1	**TS2**	**TS3**
State	$^2A'$	$^2A'$	$^2A'$
Symmetry	C_s	C_s	C_s
Rel. Energy (kcal mol^{-1})	18.5	63.8	60.1
Bond Lengths (Å) [b]			
C_1C_2	1.2064	1.3377	1.2805
C_2B	1.5047	1.4334	1.4636
C_1B	2.0924	1.7542	1.5194
BO	1.2222	1.2470	
C_2O			1.3503
Angles (°)[b]			
C_1C_2B	100.45	78.47	66.86
C_2BO	175.05	121.25	
C_2C_1O			127.56

[a] Energy calculated at UMP4STDQ/aug-cc-pVTZ//UMP2(full)/6-31G(d) level of theory and includes scaled (0.9661[37]) zero-point correction. [b] UMP2(full)/6-31G(d) level of theory.

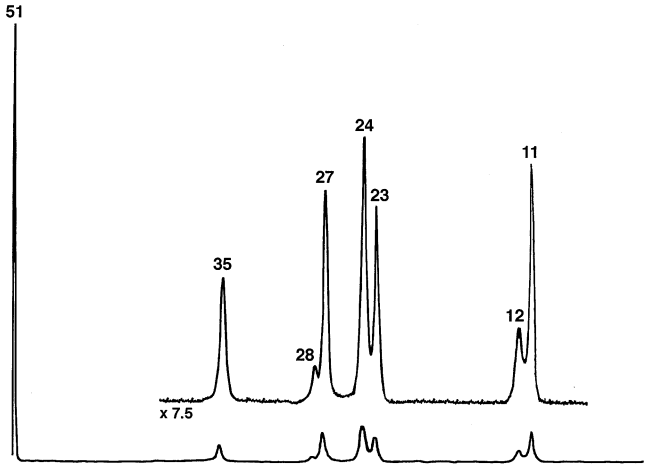

Figure 2. $^-CR^+$ spectrum of $[CCBO]^-$. Full experimental conditions see Experimental Section.

intermediate **12** (+ 58.2 kcal mol^{-1}). The overall process is endothermic by only 3.8 kcal mol^{-1}, but an excess energy of $\geq$63.8 kcal mol^{-1} is required to surmount TS2 (see Figure 1). For this process to occur, CCBO would need 53.1 kcal mol^{-1} of excess energy in addition to the Franck−Condon energy of 10.7 kcal mol^{-1}. This energy demand is high: accordingly, oxygen migration following neutralization seems unlikely. In contrast, the interconversion of CCBO to cyclic **7** has a barrier of only 18.5 kcal mol^{-1}, which means that CCBO needs 7 kcal mol^{-1} of excess energy above the Franck−Condon energy to enable this interconversion to occur. Although **7** may be accessible upon vertical oxidation of $[CCBO]^-$, it will only be a minor product. Even if **7** is formed initially in reasonable yield, it will be in equilibrium with CCBO within the microsecond time frame of the NR procedure, and since CCBO is 7.2 kcal mol^{-1} lower in energy than **7**, the proportion of **7** in an equilibrium mixture will be very small.

The $^-CR^+$and $^-NR^+$ spectra of $[CC^{11}BO]^-$ are shown in Figures 2 and 3, respectively. The recovery signal at *m*/*z* 51 dominates the $^-NR^+$ spectrum, indicating that the parent neutral (or neutrals) are particularly stable for the period between formation in the first collision cell and ionization in the second cell (10^{-6} s). Fragment peaks observed in the $^-NR^+$ spectrum

TABLE 4: Optimized Minima on the Singlet and Triplet Cation Potential Energy Surfaces

	C_1C_2BO			OC_1C_2B	C_1C_2BO			OC_1C_2B
	$^3\mathbf{1}$	$^3\mathbf{7}$	$^3\mathbf{12}$	$^3\mathbf{2}$	$^1\mathbf{1}$	$^1\mathbf{7}$	$^1\mathbf{12}$	$^1\mathbf{2}$
State	$^3\Pi$	$^3B_2$	$^3A'$	$^3A'$	$^1A'$	$^1A'$	$^1A'$	$^1A'$
Symmetry	$C_{\infty v}$	C_{2v}	C_s	C_s	C_s	C_s	C_s	C_s
Rel. Energy	0.0[a]	0.0[b]	17.2	-46.8	5.2	8.5	17.9	-41.2
(kcal mol^{-1})					(0.0)[c]	(3.2)[c]	(12.7)[c]	(-46.4)[c]
Bond Lengths (Å)[c]								
C_1C_2	1.2078	1.2814	1.3166	1.3511	1.1918	1.2203	1.2849	1.3417
C_2B	1.4300	1.5760	1.5328	1.3960	1.4292	1.4183	1.4665	1.3943
C_1B		1.5760	1.6957			2.0248	1.5567	
BO	1.2920	1.3117	1.2906		1.3168	1.3146	1.4490	
C_1O			1.6486	1.1322			1.3607	1.1335
Angles (°)[c]								
C_1C_2B	180.0	66.01	72.59	179.87	179.99	99.96	68.54	179.99
C_2BO	180.0	156.01	113.19		179.99	175.31	103.89	179.99
C_2C_1O			104.98	179.97			120.37	
C_1OB			69.25				67.20	

[a] −175.44059 hartrees. Energy calculated at UMP4STDQ/aug-cc-pVTZ//UMP2(full)/6-31G(d) level of theory including scaled (0.9661[37]) zero-point correction. [b] Stationary point $^3\mathbf{7}$ possesses one low (−43 cm^{-1}) negative frequency at the UMP2(full)/6-31G(d) level of theory. [c] Relative to CCBO singlet ground state (−175.432210 hartrees). [d] UMP2(full)/6-31G(d) level of theory.

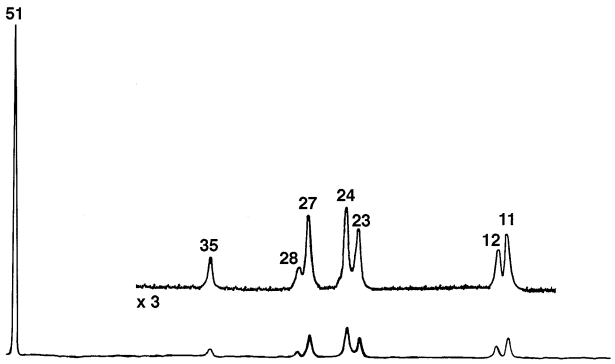

Figure 3. $^-NR^+$ spectrum of $[CCBO]^-$. Full experimental details are given in the Experimental Section.

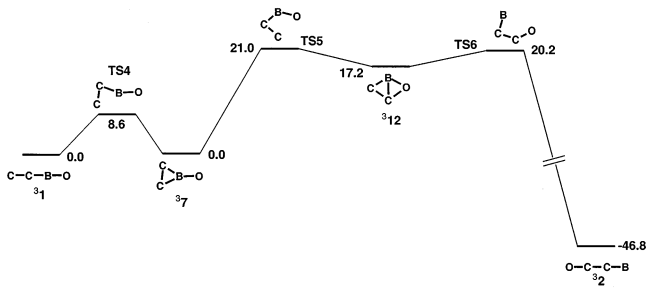

Figure 4. Rearrangement of triplet $[CCBO]^+$ to triplet $[OCCB]^+$ at the UMP4STDQ/aug-cc-pVTZ//UMP2(full)/6-31G(d) level of theory. For full details of individual structures, see Tables 4 and 5.

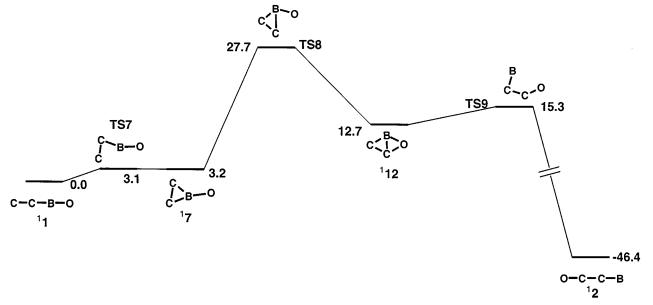

Figure 5. Rearrangement of singlet $[CCBO]^+$ to singlet $[OCCB]^+$ at the UMP4STDQ/aug-cc-pVTZ//UMP2(full)/6-31G(d) level of theory. For full details of individual structures see Tables 4 and 5.

are of small abundance, and involve the competitive losses of O, C_2, and BO, fragmentations which are in keeping with a neutral molecule of structure CCBO (such fragmentations are also consistent with cyclic structure **7**, but we have argued above that **7** is likely to be, at best, only a minor product of the vertical one-electron oxidation of $[CCBO]^-$). Interestingly, there is a smaller peak at *m*/*z* 23, corresponding to the loss of CO, a fragmentation consistent with a species of bond connectivity OCCB.[42] Whether this loss of CO is a fragmentation of neutral OCCB (cf. Figure 1) or $[OCCB]^+$ cannot be determined from $^-NR^+$ data alone.

In the $^-CR^+$ process, the anion precursor undergoes two-electron oxidation to form the cation directly (without the intermediacy of the neutral as in the $^-NR^+$ experiment). The $^-CR^+$ and $^-NR^+$ spectra are very similar to each other, and are dominated by recovery signals. Since the abundance of the peak formed by loss of CO is both small and the same in each spectrum, this must mean that the loss of CO occurs from the cation,[cf.24] which in turn means that vertical oxidation of $[CCBO]^-$ yields stable CCBO.

The Rearrangement of $[CCBO]^+$. We proposed above that the loss of CO shown in Figures 2 and 3 is a fragmentation of a decomposing cation, probably $[OCCB]^+$. The cation $[CCBO]^+$ is isoelectronic with CCCC, which is known to equilibrate its carbon atoms through the intermediacy of rhombic C_4.[21] Does $[CCBO]^+$ convert to $[OCCB]^+$ via the intermediacy of a rhombic structure? This problem has been addressed by theory (Figures 4 and 5 and Tables 4 and 5).

The triplet form of $[CCBO]^+$ is only 5.2 kcal mol^{-1} lower in energy than the corresponding singlet, and their structures are similar. Both the triplet and singlet forms of cationic $[CCBO]^+$ will be accessible following Franck−Condon oxidation from doublet CCBO since we are unable to control the energy of this process. The excess energy that the triplet cation has as a consequence of vertical Franck−Condon oxidation is calculated to be 4.8 kcal mol^{-1} whereas singlet $[CCBO]^+$ has an excess Franck−Condon energy of 8.1 kcal mol^{-1}.

The interconversions of triplet and singlet $[CCBO]^+$ to triplet and singlet $[OCCB]^+$ are shown in Figures 4 and 5, respectively. Details of geometries and energies of stable species are shown

TABLE 5: Transition States on the Singlet and Triplet Cation Potential Energy Surfaces

		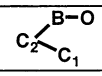	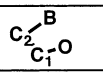	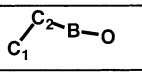	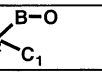	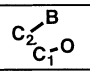
	TS4	**TS5**	**TS6**	**TS7**	**TS8**	**TS9**
State	$^3A'$	$^3A'$	$^3A'$	$^1A'$	$^1A'$	$^1A'$
Symmetry	C_s	C_s	C_s	C_s	C_s	C_s
Rel. Energy [a] (kcal mol^{-1})	8.6	21.0	20.2	8.4 (3.1)[c,d]	32.9 (27.7)[c]	20.5 (15.3)[c]
Bond Lengths (Å)[b]						
C_1C_2	1.2061	1.2835	1.3270	1.2102	1.2688	1.3197
C_2B	1.4102	1.5176	1.4914	1.4122	1.4736	1.4760
C_1B	2.1518	1.7597	1.6172	2.2040	1.7233	1.6480
BO	1.3134	1.2344		1.3131	1.2555	
C_1O			1.2578			1.2038
Angles (°)[b]						
C_1C_2B	110.42	77.34	69.75	114.16	77.47	71.99
C_2BO	178.26	128.98		178.72	129.38	
C_2C_1O			129.08			135.57

[a] Energy relative to triplet CCBO cation (−175.44046 hartrees) and calculated at UMP4STDQ/aug-cc-pVTZ//UMP2(full)/6-31G(d) level of theory and includes scaled (0.9661[37]) zero-point correction. [b] UMP2(full)/6-31G(d) level of theory. [c] Relative to singlet CCBO cation (−175.432210 hartrees). [d] Note the zero-point-energy-corrected UMP4STDQ/aug-cc-pVTZ single-point energy puts **TS7** 0.06 kcal mol^{-1} below ^{1}**7**. However, at the UMP2(full)/6-31G(d) level, at which these structures were optimized, it is 0.1 kcal mol^{-1}.

SCHEME 3

$[CCBO]^+ \rightarrow CC + BO^+$ 104.4 kcal mol^{-1}

$\rightarrow {}^4CC^{+\cdot} + BO$ 96.6 kcal mol^{-1}

$[OCCB]^+ \rightarrow BC^+ + CO$ 150.3 kcal mol^{-1}

$\rightarrow {}^4BC + CO^{+\cdot}$ 182.3 kcal mol^{-1}

in Table 4, and of transition structures in Table 5. Triplet and singlet $[OCCB]^+$ are global minima on their respective potential surfaces; the triplet is 46.8 kcal mol^{-1} below triplet $[CCBO]^+$, and the singlet 46.6 kcal mol^{-1} below singlet $[CCBO]^+$. Both rearrangement processes are significantly exothermic. The triplet and singlet rearrangements are stepwise with the maximum barriers in each being 21.0 and 27.7 kcal mol^{-1}, respectively. The triplet and singlet reactions can only proceed if additional excess energy (16.2 and 19.6 kcal mol^{-1} respectively) is available. These energies are significantly lower than that required for rearrangement of the neutral.

Experimentally, the parent cation(s) produce(s) the base peak of the $^-CR^+$ spectrum, with all peaks due to fragment ions being of small abundance as a consequence of the large endothermicities of the decomposition pathways {see Table 9 (Supporting Information) for the details of the decompositions of both singlet and triplet $[CCBO]^+$ and $[OCCB]^+$}.[43] The peaks corresponding to *m/z* 27 (BO^+) and 24 ($C_2^{+\bullet}$) [see eqs 1 and 2 for singlet decompositions (Scheme 3)] are formed by decomposition of unrearranged $[CCBO]^+$, while *m/z* 28 ($CO^{+\bullet}$) and 23 (BC^+) are characteristic of $[OCCB]^+$ [eqs 3 and 4 for singlet decompositions (Scheme 3)].[43] These data suggest that the $^-CR^+$ spectrum of $[CCBO]^-$ is composite, with contributions from both $[CCBO]^+$ and $[OCCB]^+$.

Conclusion

(i) Doublet CCBO is the major neutral formed by vertical one-electron oxidation of $[CCBO]^-$, (ii) doublet CCBO may be collisionally ionized to $[CCBO]^+$, and (iii) some of the $[CCBO]^+$ species are energized and rearrange through a distorted rhombic structure to form $[OCCB]^+$, the global minimum on the cation potential surface.

Acknowledgment. This project was supported by funding from an international link grant provided jointly by the Australian Research Council and the Deutsche Forschungsgemeinschaft and Fonds der Chemischen Industrie. S.D. and A.M.McA. acknowledge the awards of an ARC research associateship and an APRA Ph.D. scholarship, respectively. We thank APAC (Canberra) for a generous allocation of time on their supercomputing facility.

Supporting Information Available: Tables 6, 7, and 9 provide information of the thermochemistry of possible decompositions of anions, neutrals, and cations (respectively) of CCBO and OCCB. Table 8 provides details of the thermochemical data required to prepare Tables 6, 7, and 9. This material is available free of charge via the Internet at http://pubs.acs.org.

References and Notes

(1) Van Orden, A.; Saykally, R. J. *Chem. Rev.* **1998**, *98*, 2313.
(2) Verhaegen, G.; Stafford, F. E.; Droward, J. *J. Chem. Phys.* **1964**, *40* , 1622.
(3) Kouba, J. E.; Öhrn, Y. *J. Chem. Phys*. **1970**, *53* , 3923.
(4) Hirsch, G.; Buenker, R. J. *J. Chem. Phys.* **1987**, *87*, 6004.
(5) Knight, L. B.; Cobranchi, S. T.; Petty, J. T.; Earl, E.; Feller, D.; Davidson, E. R. *J. Chem. Phys.* **1989**, *90*, 690.
(6) Oliphant, N.; Adamowicz, L. *Chem. Phys. Lett.* **1990**, *168*, 126.
(7) Fernando, W. T. M. L.; O'Brien, L. C.; Bernath, P. F. *J. Chem Phys*. **1990**, *93*, 8482.
(8) Martin, J. M. L.; Taylor, P. R. *J. Chem. Phys*. **1994**, *100*, 9002.
(9) Wyss, M.; Grutter, M.; Maier, J. P. *J. Phys. Chem*. **1998**, *102*, 9106.
(10) Martin, J. M. L.; Taylor, P. R.; Yustein, J. T.; Burkholder, T. R.; Andrew, L. *J. Chem. Phys.* **1993**, *99*, 12.
(11) Presilla-Marquez, J. D.; Larson, C. W.; Carrick, P. G.; Rittby, C. M. L. *J. Chem. Phys.* **1996**, *99*, 12.
(12) Knight, L. B.; Cabranchi, S.; Earl, E. *J. Chem. Phys*. **1996**, *104*, 4927.
(13) Wang, C. R.; Huang, R. B.; Liu, Z. Y.; Zheng, L. S. *Chem. Phys. Lett.* **1995**, *242*, 355.
(14) Zhan, C. G.; Iwata, S. *J. Phys. Chem.* **1997**, *101*, 1, 591.
(15) Léonard, C.; Rosmus, P.; Wyss, M.; Maier, J. P. *Phys. Chem. Chem. Phys*. **1999**, *1*, 1827.
(16) Comeau, M.; Leleyter, M.; Leclercq, J.; Pastoli, G. *Am. Inst. Phys. Conf. Proc.* **1994**, *312*, 605.
(17) Presilla-Marquez, J. D.; Carrick, P. G.; Larson, C. W. *J. Chem. Phys.* **1999**, *110*, 5702.
(18) Hamrick, Y. M.; VanZee, R. J.; Godbout, J. T.; Weltner, W. J.; Lauderdale, W. J.; Stanton, J. F.; Bartlett, R. J. *J. Phys. Chem*. **1991**, *95*, 2840.
(19) Burkholder, T. R.; Andrews, L. *J. Phys. Chem*. **1992**, *96*, 10195.
(20) Wang, C.; Huang, R.; Liu, Z.; Zheng, L. *Chem. Phys. Lett.* **1995**, *242*, 355.

(21) Blanksby, S. J.; Schröder, D.; Dua, S.; Bowie, J. H.; Schwarz, H. *J. Am. Chem. Soc.* **2000**, *122* , 7105.

(22) Sheldon, J. C.; Currie, G. J.; Bowie, J. H. *J. Am. Chem. Soc*. **1988**, *110*, 8266.

(23) Wesdemiotis, C.; McLafferty, F. W. *Chem. Rev*. **1987**, *87*, 485.

(24) Schalley, C. A.; Hornung, G.; Schröder, D.; Schwarz, H. *Int. J. Mass Spectrom. Ion Processes* **1998**, *172*, 181. Schalley, C. A.; Hornung, G.; Schröder, D.; Schwarz, H. *Chem. Soc. Rev*. **1998**, *27*, 91.

(25) Zagorevskii, D. V.; Holmes, J. L. *Mass Spectrom. Rev.* **1999**, *18*, 87.

(26) DePuy, C. H.; Bierbaum, V.; Flippin, L. A.; Grabowski, J. J.; King, G. K.; Smitt, R. J.; Sullivan, S. A. *J. Am. Chem. Soc.* **1980**, *102*, 5012.

(27) Wenthold, P. G.; Hu, J.; Squires, R. R. *J. Am. Chem. Soc.* **1994**, *116*, 6961.

(28) Holmes, J. L. *Org. Mass Spectrom.* **1985**, *20*, 169.

(29) Bowie, J. H.; Blumenthal, T. *J. Am. Chem. Soc.* **1975**, *97*, 2959.

(30) Szulejko, J. E.; Bowie, J. H.; Howe, I.; Beynon, J. H. *Int. J. Mass Spectrom. Ion Phys.* **1980**, *13*, 76.

(31) Bursey, M. *Mass Spectrom. Rev.* **1990**, *9*, 555.

(32) Hornung, G.; Schalley, C. A.; Dieterle, M.; Schröder, D.; Schwarz, H. *Chem. Eur. J*. **1997**, *3*, 1866.

(33) Schalley, C. A.; Blanksby, S. J.; Harvey, J. N.; Schröder, D.; Zummack, W.; Bowie, J. H.; Schwarz, H. *Eur. J. Org. Chem*. **1998**, 987.

(34) Brown, H. C.; Bhat, N. G.; Srebnik, M. *Tetrahedron Lett*. **1988**, *29*, 2631.

(35) Brown, C. D.; Chong, J. M.; Shen, L. *Tetrahedron* **1999**, *55*, 14233.

(36) Frisch, M. J.; Trucks, G. W.; Schlegel, H. B.; Scuseria, G. E.; Robb, M. A.; Cheeseman, J. R.; Zakrzewski, V. G.; Montgomery, J. A.; Stratmann, R. E.; Burant, J. C.; Dapprich, S.; Millam, J. M.; Daniels, A. D.; Kudin, K. N.; Strain, M. C.; Farkas, O.; Tomasi, J.; Barone, V.; Cossi, M.; Cammi, R.; Mennucci, B.; Pomelli, C.; Adama, C.; Clifford, S.; Ochterski, J.; Morokuma, B.; Malich, D. K.; Rabuck, A. D.; Raghavachari, K.; Foresman, J. B.; Cioslowski, J.; Ortiz, J. V.; Stefanov, B. B.; Liu, G.; Liashenko, A.; Piskorz, P.; Komaromi, I.; Gomperts, R.; Martin, R. L.; Fox, D. J.; Keith, T.; Al-Laham, M. A.; Peng, C. Y.; Nanayakkara, A.; Gonzalez, C.; Challacombe, M.; Gill, P. M. W.; Johnson, B. G.; Chen, W.; Wong, M. W.; Andres, J. L.; Head-Gordon, M.; Replogle, E. S.; Pople, J. A. *Gaussian 98*; Gaussian, Inc.: Pittsburgh, PA, 1998.

(37) Scott, A. P.; Radom, L. *J. Phys. Chem*. **1996**, *100*, 16502.

(38) Dunning, T. H. *J. Chem. Phys*. **1989**, *90*, 1007.

(39) Woon, D. E.; Dunning, T. H. *J. Chem. Phys.* **1993**, *98*, 1358.

(40) It is unlikely that the last step of this reaction involves an S_N2 process; the bulky *iso*-Pr group favors elimination rather than substitution.

(41) A reviewer has asked whether it is possible that some $[CCBO]^-$ ions are "metastable" with respect to electron loss. This seems unlikely since the adiabatic electron affinity of CCBO is 4.8 eV (Table 1). Even so, we have carried out the following experiment to answer this question. The parent anion $[CCBO]^-$ is fired through the first collision cell which contains no collision gas. The deflector between the two cells is charged, and the second cell contains O_2. Only neutrals formed by "metastable" electron loss from $[CCBO]^-$ can enter the second collision cell. No positive ions signals were detected from this $[^-$("metastable" N)$R^+]$ experiment.

(42) Calculated energies for decomposition processes of these neutrals are recorded in Table 7 (Supporting Information). Energies and geometries of fragment neutrals are given in Table 8 (Supporting Information).

(43) In Scheme 3 and Tables 6, 7, and 9, the spin states are not indicated except for triplet or quartet states.